Pulse quality analysis on soliton pulse compression and soliton self-frequency shift in a hollow-core photonic bandgap fiber

N. González-Baquedano,[1,*] I. Torres-Gómez,[1] N. Arzate, [1] A. Ferrando,[2] and D. E. Ceballos-Herrera[3]

[1]*Centro de Investigaciones en Óptica A.C., Loma del Bosque 115, Lomas del Campestre, 37150, León, Guanajuato, México*
[2]*Departamento de Óptica, Universidad de Valencia, Dr. Moliner 50, Burjassot 46100, Valencia, Spain*
[3]*Universidad Autónoma de Nuevo León, Facultad de Ciencias Físico Matemáticas (FCFM), CICFIM, Av. Universidad s/n, Cd. Universitaria, San Nicolas de los Garza, 66451, Nuevo León, México.*
[*]*noegb@cio.mx*

Abstract: A numerical investigation of low-order soliton evolution in a proposed seven-cell hollow-core photonic bandgap fiber is reported. In the numerical simulation, we analyze the pulse quality evolution in soliton pulse compression and soliton self-frequency shift in three fiber structures with different cross-section sizes. In the simulation, we consider unchirped soliton pulses (of 400 fs) at the wavelength of 1060 nm. Our numerical results show that the seven-cell hollow-core photonic crystal fiber, with a cross-section size reduction of 2%, promotes the pulse quality on the soliton pulse compression and soliton self-frequency shift. For an input soliton pulse of order 3 (which corresponds to an energy of 1.69 μJ), the pulse gets compressed with a factor of up to 5.5 and a quality factor of 0.73, in a distance of 12 cm. It also experiences a soliton-self frequency shift of up to 28 nm, in a propagation length of 6 m, with a pulse shape quality of ≈ 0.80.

OCIS codes: (190.5530) Pulse propagation and temporal solitons; (060.5295) Photonic crystal fibers; (190.4370) Nonlinear optics, fibers.

References and links

1. J. C. Knight, "Photonic crystal fibres," Nature **424,** 847–851 (2003).
2. D. G. Ouzounov, C. J. Hensley, A. L. Gaeta, N. Venkataraman, M. T. Gallagher, and K. W. Koch, "Soliton pulse compression in photonic band-gap fibers," Opt. Express **13,** 6153–6159 (2005).
3. F. Gérôme, K. Cook, A. K. George, W. Wadsworth, and J. C. Knight, "Delivery of sub-100fs pulses through 8m of hollow-core fiber using soliton compression," Opt. Express **15,** 7126–7131 (2007).
4. D. G. Ouzounov, F. R. Ahmad, D. Müller, N. Venkataraman, M. T. Gallagher, M. G. Thomas, J. Silcox, K. W. Koch, and A. L. Gaeta, "Generation of megawatt optical solitons in hollow-Core photonic band-gap fibers," Science **301,** 1702–1704 (2003).
5. F. Luan, J. C. Knight, P. S. J. Russell, S. Campbell, D. Xiao, D. T. Reid, B. J. Mangan, D. P. Williams, and P. J. Roberts, "Femtosecond soliton pulse delivery at 800 nm wavelength in hollow-core photonic bandgap fibers," Opt. Express **12,** 835–840 (2004).
6. D. V. Skryabin, "Coupled core-surface solitons in photonics crystal fibers," Opt. Express **12,** 4841–4846 (2004).

#183383 - $15.00 USD Received 11 Jan 2013; revised 13 Mar 2013; accepted 14 Mar 2013; published 5 Apr 2013

7. J. C. Knight, F. Gérôme, and W. J. Wadsworth, "Hollow-core photonic crystal fibres for delivery and compression of ultrashort optical pulses," IEEE J. Quantum Electron. **39,** 1047–1056 (2007).
8. J. Lægsgaard and P. J. Roberts, "Dispersive pulse compression in hollow-core photonic band gap fibers," Opt. Express **16,** 9268–9644 (2008).
9. J. Lægsgaard, "Soliton formation in hollow-core photonic bandgap fibers," Appl. Phys. B **95,** 2093–3000 (2009).
10. M. G. Welch, K. Cook, R. A. Correa, F. Gerome, W. J. Wadsworth, A. V. Gorbach, D. V. Skryabin, and J. C. Knight, "Solitons in hollow core photonic crystal fiber: engineering nonlinearity and compressing pulses," J. Lightwave Technol. **27,** 1644–1652 (2009).
11. A. A. Ivanov, A. A. Podshivalov, and A. M. Zheltikov, "Frequency-shifted megawatt soliton output of a hollow photonic-crystal fiber for time-resolved coherent anti-Stokes Raman scattering microspectroscopy," Opt. Lett. **31,** 3318–3320 (2006).
12. B-W. Liu, M-L. Hu, X-H. Fang, Y-F. Li, L. Chai, C-Y. Wang, W. Tong, J. Luo, A. A. Voronin, and A. M. Zheltikov, "Stabilized soliton self-frequency shift and 0.1-PHz sideband generation in a photonic-crystal fiber with an air-hole-modified core," Opt. Express **16,** 14987–14996 (2008).
13. F. Gérome, P. Dupriez, J. Clowes, J. C. Knight, and W. J Wadsworth, "High power tunable femtosecond soliton source using hollow-core photonic bandgap fiber, and its use for frequency doubling," Opt. Express **16,** 2381–2386 (2008).
14. A. V Gorbach and D. V Skryabin, "Soliton self-frequency shift, non-solitonic radiation and self-induced transparency in air-core fibers," Opt. Express **16,** 4858–4865 (2008).
15. N. González-Baquedano, N. Arzate, I. Torres-Gómez, A. Ferrando, D. E. Ceballos-Herrera, and C. Milián, "Femtosecond pulse compression in a hollow-core photonic bandgap fiber by tuning its cross section," Photonics and Nanostructures – Fundamentals and Applications **10,** 594–601 (2012).
16. R. Amezcua-Correa, N. G. Broderick, M. N. Petrovich, F. Poletti, and D. J. Richardson, "Optimizing the usable bandwidth and loss through core design in realistic hollow-core photonic bandgap fibers," Opt. Express **14,** 7974–7985 (2006).
17. G. P. Agrawal, *Non-Linear Fiber Optics* (Academic, 2007).
18. C. J. Hensley, D. G. Ouzounov, and A. L. Gaeta, "Silica-glass contribution to the effective non-linearity of hollow-core photonic band-gap fibers ," Opt. Express **15,** 3507–3512 (2007).
19. J. Lægsgaard, J. Riishede, A. Bjarklev, and N. A. Mortensen, "Material effects in air-guiding photonic band gap fibers," J. Opt. Soc. Am. B **20,** 2046–2051 (2003).
20. N. González Baquedano, S. Vargas, N. Arzate, I. Torres-Gómez, A. Martínez-Ríos, D. E. Ceballos-Herrera, A. Ferrando, and C. Milián, "Modeling the tapering effects on the modal parameters of a hollow-core photonic bandgap fiber," in *Eight Symposium Optics in Industry,* E. Rosas, N. Arzate, I. Torres and J. Sumaya, eds., Proc. SPIE **8287,** 828701 (2011).
21. F. Poli, A. Cucinotta, and S. Selleri, *Photonic Crystal Fibers* (Springer, 2007).
22. J. M. Dudley, G. Genty, and S. Coen, "Supercontinuum generation in photonic crystal fiber," Rev. Mod. Phys. **78,** 1135–1184 (2006).
23. E. M. Dianov, Z. S. Nikonova, A. M. Prokhorov, and V. N. Serkin, "Optimal compression of multi-soliton pulses in optical fibers," Sov. Tech. Phys. Lett. **12,** 311–313 (1986).
24. G. P. Agrawal, *Applications of Nonlinear Fiber Optics* (Academic, 2001).
25. K-T. Chai and W-H. Cao, "Enhanced compression of fundamentals solitons in dispersion decreasing fibers due to the combined effects of negative third-order dispersion and Raman self-scattering," Opt. Commun. **184,** 463–474 (2000).

1. Introduction

Nowadays hollow-core photonic bandgap fibers (HC-PBGFs) and non-linear phenomena such as soliton pulse compression (SPC) and soliton self-frequency shift (SSFS) are in continuous investigation [1–3]. The interest of the scientific community has been focused on the development of new technologies of light sources and applications based almost entirely in such kind of fibers. Several research groups have made important advances both experimentally and theoretically in the understanding of soliton compression and soliton formation as well as its dynamics in HC-PBGFs [4–6]. Recently, in the study of SPC, Ouzounov et al. successfully compressed a 120 fs input pulse into 50 fs pulse by using a 24 cm Xe-filled HC-PBGF [2]. Gérôme et al. also reported the existence of soliton compression. They achieved output pulses of 90 fs from 195 fs input pulses by using 8 m of tapered fiber [3, 7]. Lægsgaard and Roberts studied numerically the soliton formation during the compression of chirped gaussian pulses in HC-PBGFs. They concluded that the third-order dispersion, TOD, is a crucial parameter that

#183383 - $15.00 USD Received 11 Jan 2013; revised 13 Mar 2013; accepted 14 Mar 2013; published 5 Apr 2013

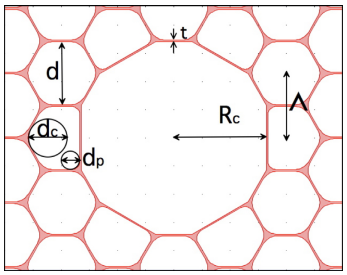

Fig. 1. Cross section of the modeled HC-PBGF. The colored (white) areas indicate silica (air) regions [15].

prevents the formation of shorter soliton pulses [8, 9]. Welch and collaborators demonstrated a temporal compression factor of 12, in a seven-cell hollow-core tapered fiber with a length of 35 m, for picosecond input pulses [10].

On the other hand, SSFS and their applications have also been studied [11, 12]. Ouzounov et al., for instance, reported a SSFS from 1470 nm to 1530 nm [4]. Making use of such phenomenon, Gérôme reported a high power tunable femtosecond soliton source of 33 nm wavelength tuneability [13]. Gorbach and Skryabin studied the dynamics that accompany the soliton propagation in the femtosecond regime in HC-PBGFs. Their model included non-linear responses of both the silica, in the cladding, and of the air. They concluded that the strong Raman response of air does not always result in a large SSFS in HC-PBGFs [14].

Although SPC and SSFS have been studied, those studies lack of an analysis of the quality of the output pulse. In a recent paper, we studied numerically the effects of tuning the cross-section size of a HC-PBGFs on the modal parameters in order to have a fiber structure which promotes pulse compression. The study includes an analysis of the pulse shape quality of the compressed pulse as it propagates along the fiber [15]. In this paper, we apply such kind of analysis in order to study the pulse quality in both phenomena SPC and SSFS. Firstly, we study the impact of tuning the cross section size of the HC-PBGF on the modal parameters. Secondly, for the studied HC-PBGF, we present a numerical study of low-order soliton evolution by solving the generalized non-linear Schrödinger equation. In particular, we focus on finding a HC-PBGF structure that promotes an improvement of the pulse quality of both the compressed and the shifted soliton pulse. In the calculation, we consider an initial input pulse at a wavelength of $\lambda_0 = 1060$ nm. We also take into account contributions of air and silica to the non-linear parameter, the interplay of the effects of second- and third-order dispersion and the intrapulse stimulated Raman scattering. Higher-order dispersion terms are neglected since the described spectral evolution takes place away from the zero group-velocity dispersion (GVD) [14]. According to the author's best knowledge, this is the first report of an analysis of the pulse quality on SPC and SSFS in HC-PBGFs.

2. Theory and numerical procedure

The modeled HC-PBGF structure consists of a triangular lattice of rounded hexagonal holes and an air core formed by seven-missing hexagonal unit cells as it is shown in Fig. 1. The fiber transmission behavior is ruled by its geometry parameters, such as the hole diameter, d, the pitch, Λ, the diameter of curvature at the corners, d_c, the circle diameter, d_p, the silica ring thickness, t, and the core size, R_c. The core design of the fiber has a direct impact on the modal properties of the fiber. In this way, the rounded hexagonal holes in the structure of the fiber were chosen mainly for two important reasons: firstly, they increase the width of the transmission band of HC-PBGFs [16], and, secondly, their shape is typically that founded in

#183383 - $15.00 USD Received 11 Jan 2013; revised 13 Mar 2013; accepted 14 Mar 2013; published 5 Apr 2013

commercial fibers. We find the fundamental guided mode and its respective effective refractive index for HC-PBGFs with three different cross-section sizes. Once the effective refractive index of the mode is obtained, we compute their corresponding dispersion and non-linear parameters. The former can be computed expanding the propagation constant, $\beta(\omega)$, around the central frequency ω_0 as [17]

$$\beta(\omega) = \beta(\omega_0) + \beta_1(\omega_0)\Omega + (1/2)\beta_2(\omega_0)\Omega^2 + (1/6)\beta_3(\omega_0)\Omega^3 + ..., \tag{1}$$

where $\Omega = \omega - \omega_0$, and

$$\beta_k(\omega_0) = \left.\frac{d^k\beta}{d\omega^k}\right|_{\omega_0} \tag{2}$$

are the k-order dispersion parameters. The dispersion slope is quantified by the figure of merit, RDS, given by the ratio [9]:

$$\mathrm{RDS} = \frac{\beta_3}{|\,\beta_2\,|}, \tag{3}$$

which has dimensions of time.

Although the core of the fiber is made of air, the non-linear parameter of the HC-PBGFs does not only arise from the contribution of the air but also from the contribution of the silica [18,19]. This is because part of the guided mode also overlaps with regions made of silica. Therefore it is important to include both contributions, that of the air and that of the silica, on the non-linear parameter to the propagation equation. The non-linear parameter of the material can be calculated from [17]:

$$\gamma_i = \frac{2\pi n_2^i}{\lambda A_{eff}^i}, \tag{4}$$

where i can be a or s referring to air or silica, respectively. n_2^i and A_{eff}^i are the non-linear refractive index and the effective area of the i-th material, correspondingly [20]. The total contribution of the non-linear parameter is given by [21]:

$$\gamma_T = \gamma_a + \gamma_s. \tag{5}$$

Once the dispersion and non-linear parameters are obtained, we are able to study the evolution of low-order solitons in HC-PBGFs. We use the generalized non-linear Schrödinger equation which describes the propagation of light pulses in optical fibers. We consider the inclusion of second- (β_2) and third-order (β_3) dispersion, as well as non-linear response (γ) and intra-pulse stimulated Raman scattering terms on the Schrödinger equation. The propagation equation is numerically solved by using the symmetric split-step Fourier method. For the non-linear response and Raman function, we take into account their corresponding contributions of the silica and of the air [14], that is

$$\begin{aligned}\frac{\partial A}{\partial z} + \frac{i}{2}\beta_2\frac{\partial^2 A}{\partial t^2} - \frac{1}{6}\beta_3\frac{\partial^3 A}{\partial t^3} &= i\gamma_a(1-f_a)\,|\,A\,|^2 A + i\gamma_s(1-f_s)\,|\,A\,|^2 A \\ + i\gamma_a f_a A\int_{-\infty}^{+\infty} dt' R_a(t')\,|\,A(t-t',z)\,|^2 &+ i\gamma_s f_s A\int_{-\infty}^{+\infty} dt' R_s(t')\,|\,A(t-t',z)\,|^2,\end{aligned} \tag{6}$$

where $A = A(t,z)$ is the slowly-varying pulse envelope in a co-moving frame and z is the spatial coordinate along the fiber. The corresponding contributions to the Raman response function due to air, R_a, and silica, R_s, are described by [17]:

$$R_i(t) = \Theta(t)\frac{(\tau_1^{(i)})^2 + (\tau_2^{(i)})^2}{\tau_1^{(i)}(\tau_2^{(i)})^2}\exp\left[-t/\tau_2^{(i)}\right]\sin\left(t/\tau_1^{(i)}\right), \tag{7}$$

#183383 - $15.00 USD Received 11 Jan 2013; revised 13 Mar 2013; accepted 14 Mar 2013; published 5 Apr 2013

where $\Theta(t)$ is the Heaviside function, τ_1 and τ_2 are the Raman parameters, which values for silica are well known and have the following values [17]: $\tau_1^s = 12.2\,\text{fs}$, $\tau_2^s = 32\,\text{fs}$ and $f_s = 0.18$. Meanwhile, the estimated values for air are [14] $\tau_1^a = 62\,\text{fs}$, $\tau_2^a = 77\,\text{fs}$ and $f_a = 0.5$.

Losses are neglected. Furthermore effects such as self-steepening, two-photon absorption and plasma generation have also been neglected in the model because it is assumed that the described spectral evolution takes place away from the zero GVD, wherein such phenomena are no significant [14].

During the pulse propagation, a soliton is formed when the anomalous dispersion and the non-linear effects (self-phase modulation) in the medium of propagation are mutually compensated. The order of the soliton is given by: $N^2 = (t_0^2 \gamma_T P_0)/|\beta_2|$, where t_0 is the pulse width and P_0 is the peak power. The fundamental optical soliton (with order $N = 1$) is a light pulse whose temporal and spectral profiles does not change with propagation. If a higher-order, $N > 1$, soliton propagates along the fiber, it undergoes stages of periodical compression and broadening of its temporal and spectral shape. However, in the presence of perturbation, the higher-order soliton breaks up into lower amplitudes sub-pulses. Such break up is known as soliton fission. In the femtosecond regime, higher-order dispersion and Raman scattering are the main effects that causes soliton fission. The distance at which fission starts usually corresponds to the point where the evolving input higher-order soliton reaches its maximum bandwidth [22]. It is one of our interest to find an optimum length at which a higher order soliton reaches its minimum temporal width along with a high-quality shape. Such an optimum length, z_{opt}, is predicted by the following equation [23]:

$$z_{opt} = \frac{\pi}{2}\left[\frac{0.32}{N} + \frac{1.1}{N^2}\right] L_D, \tag{8}$$

where L_D is the dispersion length [17]. The pulse compression is quantified by the compression factor defined by [24]:

$$F_C = \frac{t_{FWHM}}{t_{comp}}, \tag{9}$$

where t_{FWHM} and t_{comp} are the full-width at half maximum (FWHM) of the input and output compressed pulse, respectively.

The pulse quality is quantified by quality factor,

$$Q_c = 1 - \frac{E_{\text{pedestal}}}{100}, \tag{10}$$

which gives the fraction of energy that is contained in the output pulse with respect to that of the input pulse. E_{pedestal} is the pedestal energy that gives the percentage of the total input energy that is contained in the pedestal of the output (either compressed or shifted) pulse. It is defined as [25]:

$$E_{\text{pedestal}} = \frac{|\, E_{\text{total}} - E_{\text{sech}}\,|}{E_{\text{total}}} \times 100, \tag{11}$$

where E_{total} is the total energy contained in the output pulse and E_{sech} is the energy of a hyperbolic-secant pulse having the same peak power and FWHM as the output pulse.

In our analysis, we consider a hyperbolic secant input pulses in the form of

$$A(t,0) = \sqrt{P_0}\,\text{sech}\,(t/t_0), \tag{12}$$

where the peak power takes values in such a way that the corresponding input soliton orders are $N = 2, 2.5, 3$ and $t_0 = 400\,\text{fs}$ is the input pulse width.

#183383 - $15.00 USD Received 11 Jan 2013; revised 13 Mar 2013; accepted 14 Mar 2013; published 5 Apr 2013

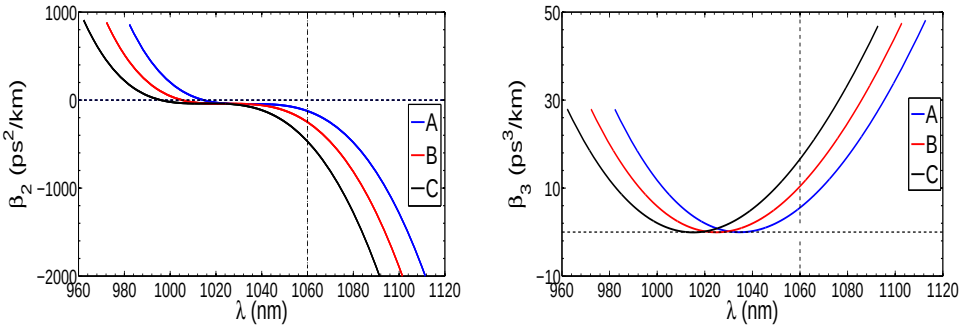

(a) (b)

Fig. 2. Second- (a) and third-order (b) dispersion parameters as a function of wavelength for the A, B and C structures.

3. Results and discussion

We studied three HC-PBGF structures, namely A, B and C. The A fiber structure has the main initial parameters: $d = 2.46$ μm, $\Lambda = 2.53$ μm, $d_p = 0.66$ μm, $d_c = 1.32$ μm and $R_c = 3.61$ μm. Meanwhile, the cross-section size of the B and C fiber structures have been reduced to 1 and 2 %, respectively, with respect to that of the A structure. In other words, we consider that the fiber preserves its original form and geometry and only experiences an uniform decrease of its transversal dimensions. Second- and third-order dispersion parameters as a function of wavelength for such structures are depicted in Fig. 2. The transmission bandwidth is ≈ 130 nm. Most of the allowed wavelengths are in the anomalous region. The zero-dispersion wavelengths (ZDWs) for the studied HC-PBGFs are located at 1015, 1005 and 995 nm, respectively. In addition, the second-order dispersion parameter values, for the A, B, and C fiber structures, at $\lambda_0 = 1060$ nm, are the following: -120, -245 and -457 ps^2/km, respectively. As expected, the effect of reducing the cross-section size of the HC-PBGF is the shift of the ZDW to shorter wavelengths and, consequently, the second-order dispersion takes more negative values Fig. 2(a). From Fig. 2(b), it can be seen that β_3 presents the same qualitative behavior for the three structures. TOD curves shift to shorter wavelengths and the value of β_3 at 1060 nm gets increased as the cross-section size of the fiber is reduced. Their corresponding β_3 values are the following: 5, 10 and 16 ps^3/km, respectively. The respective energy of input solitons with orders N =2, 2.5 and 3 are: 223.1 nJ, 348.6 nJ and 501.98 nJ, for the A fiber structure; 426 nJ, 666.51 nJ and 960 nJ, for the B fiber structure; and 0.751 μJ, 1.173 μJ and 1.69μJ for the C fiber structure, respectively.

We can see from Fig. 3 the silica and air contributions to the total non-linear parameter as a function of wavelength for the HC-PBGF A structure. Similar behavior of the nonlinear parameter for the B and C structure is observed. A reduction of the cross-section size of the fiber of 1% and 2% induces an increment of the magnitude of γ_T, at the wavelength of 1060 nm, of 0.057×10^{-5} and 0.131×10^{-5} $1/(\mathrm{W}\cdot\mathrm{km})$, respectively. We observe that the main contribution to the non-linear parameter comes from the air region. The principal feature of γ_T, seen in all corresponding curves, is the almost flat region that is present in the middle of the transmission bandwidth. In addition, there is an increase in both the low and the upper sides of the respective curves. Besides, γ_T takes higher values as the cross-section size is reduced.

Figure 4 shows the relative dispersion slope for the three studied HC-PBGFs as a function of wavelength. It can be observed that the reduction of the cross-section size of the HC-PBGF produces lower values for the RDS and a decrease of the wavelength range, within the anomalous

#183383 - $15.00 USD Received 11 Jan 2013; revised 13 Mar 2013; accepted 14 Mar 2013; published 5 Apr 2013

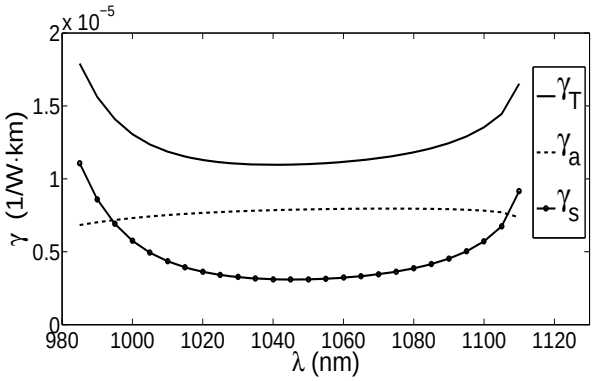

Fig. 3. Non-linear parameters contributions for the studied HC-PBGFs A structure as a function of wavelength. The total non-linear parameter, γ_T, is given by the sum of the contributions of the silica, γ_s, and of the air, γ_a.

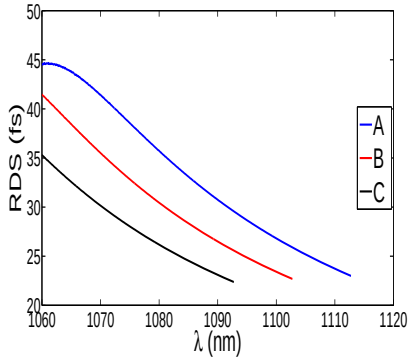

Fig. 4. Relative dispersion slope, RDS, as a function of wavelength, for the three studied HC-PBGFs.

region, wherein the input pulse can propagate. The latter can be understood recalling that the transmission window is shifted to shorter wavelengths due to the reduction of the cross-section size of the HC-PBGF, as it can be seen from Fig. 2. The transmission wavelength ranges are $\approx$ 52, 42 and 32 nm for the A, B and C fiber structures, respectively.

We study the evolution of a soliton pulse of order N, as it propagates along the HC-PBGF taking into account the effects of second- and third-order dispersion, self-phase modulation and intra-pulse Raman scattering. During the propagation, the pulse experiences an initial stage of compression (or a broadening of the spectrum) and, after some distance it reaches maximum compression (or maximum bandwidth), which corresponds to the optimum length, z_{opt}, that indicates the onset of the soliton fission. The resultant sub-pulse undergoes stages of compression and broadening experiencing a continuous shift to longer wavelengths due to the Raman gain [22]. Then it follows the formation of a fundamental soliton which central wavelength keeps redshifting as it propagates along the fiber. This behavior can be seen, in detail, in Fig. 5, which shows density plots for the temporal and spectral evolution of an input soliton pulse, of order $N = 2$, as it propagates along ten meters of the A HC-PBGF. In the following, we will study both the temporal and spectral evolution of a soliton pulse. Firstly, we will study the optimum compressed soliton pulse and, secondly, the maximum soliton self-frequency shift.

#183383 - $15.00 USD Received 11 Jan 2013; revised 13 Mar 2013; accepted 14 Mar 2013; published 5 Apr 2013

Figure 6 shows the compression factor experienced for the soliton pulse as it propagates through the different studied HC-PBGFs. The soliton pulse propagates and undergoes a first stage of compression in which it reaches a minimum temporal width at the optimum length, z_{opt} [see Eq. 8]. Later, a second stage is observed, in which there is an oscillatory behavior of compression and broadening of the pulse width; and, finally, it follows a decreasing tendency indicating the formation of a fundamental soliton which is fissioned from the input pulse. We can also observe from Figs. 6(a)-6(c) that the maximum compression factor increases with a higher value of the soliton order. Furthermore, we point out that the maximum values of the compression factor of the pulse in all three studied HC-PBGFs are approximately equal but the propagation length at which those values are reached decreases as the soliton order increases, and the cross-section size of the fiber is reduced (or for those structures with larger negative values of β_2).

Figure 7 shows the quality factors of the pulse as it propagates along the three HC-PBGFs. The behavior of the quality factor is such that it firstly decreases to a minimum value; then it experiences an oscillatory stage and, after certain distance, it almost keeps a constant value. The first two stages correspond to the stages of compression and broadening of the initial pulse. Meanwhile, in the last stage, the formation of a fundamental soliton takes place. Another feature seen in Fig. 7 is that higher-order input solitons results in, as an average, a general decrease of the quality factor, and a decrease of the distance at which the fundamental soliton is formed. For input solitons with orders of $N = 2, 2.5$ and 3, the quality factors of the redshifted solitons is ≈ 0.9, 0.85 and 0.8, respectively. Since, for higher-order input solitons, their quality factors are negatively affected, we only present results for up to $N = 3$. It can be seen, from both Fig. 7 and Fig. 6, that in order to achieve higher compression factors, it is necessary to increase the value of the soliton order. However, by doing so, it results in a decrease of the quality of the compressed pulse.

This can be seen clearly in Fig. 8 where the temporal evolution of the pulse as well as the optimum output compressed pulse as a function of soliton order for the HC-PBGF C structure are depicted. Considering an input pulse with a value of the soliton order of $N = 2$, the compression factor reaches a value of 3.3, in 23 cm, with a pulse quality factor of 0.88. Meanwhile, for an input soliton pulse of $N = 3$, its F_C increases until 5.6, in 12 cm; however, the pulse quality factor decreases to a value of 0.73. Similar behavior is observed for the compressed pulses for the A and B fiber structures. Table 1 summarizes the results obtained for the SPC in the three studied HC-PBGFs structures.

We can observe, in Figs. 9(a)-9(c), the spectra of the output-pulse power after 10 m of propa-

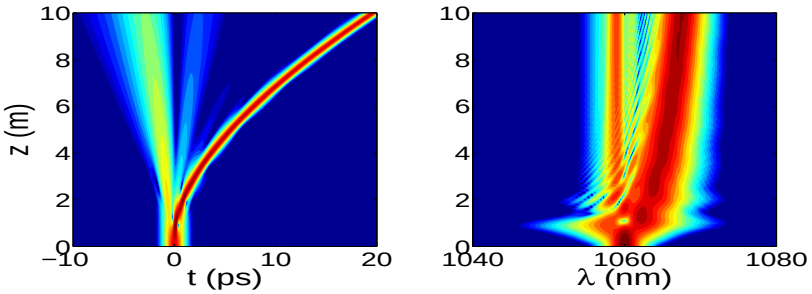

Fig. 5. Density plots of the temporal (a) and spectral (b) evolution of an input soliton pulse of order $N = 2$, along a propagation length of ten meters, in a HC-PBGF.

#183383 - $15.00 USD Received 11 Jan 2013; revised 13 Mar 2013; accepted 14 Mar 2013; published 5 Apr 2013

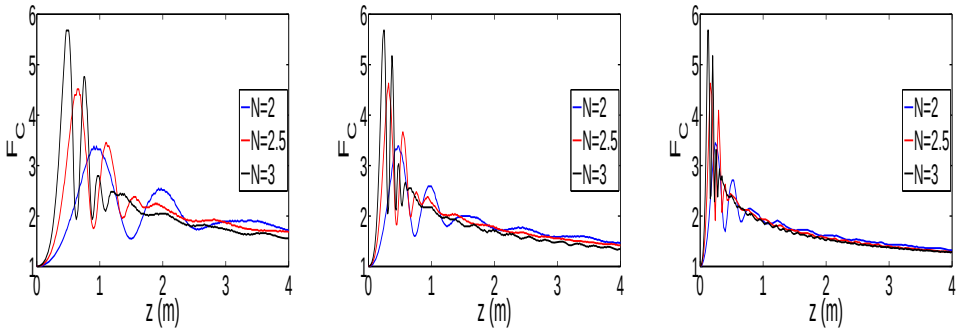

(a) (b) (c)

Fig. 6. Compression factor as a function of the propagation length and of soliton number, N, for the studied HC-PBGFs: (a) A, (b) B, and (c) C .

gation length for the A structure. If the input soliton number increases, the SSFS also does. For the A fiber structure, the soliton of order $N = 3$ reaches a central wavelength of $\lambda_0 = 1076.5$ nm.

In Figs. 9(d)-9(f), upper panels, the spectra of the output-pulse density for the C fiber structure can be seen. The soliton of order $N = 3$ reaches the largest SSFS after a propagation length of 6 m: $\lambda_0 = 1088.4$ nm. Such an improvement can be understood if we recall that the C structure presents higher values for its non-linear parameter than those corresponding to the A and B fiber structures. We can also see from Figs. 9(d)-9(f), lower panels, that the higher value of the soliton order, the larger initial shift of the fundamental soliton is. After an initial stage of accelerated soliton redshift, it decelerates to a lower value. For example: for $N = 2$, after a propagation length of 5 m, the fundamental soliton redshifts 11.6 nm; meanwhile, in the following 5 m of propagation, it only redshifts 3.2 nm. We underline that, according to our results, if the soliton order is increased, the SSFS also does. Table 2 lists the output parameters of soliton self-frequency shift for input soliton pulses of order $N = 2, 2.5, 3$, respectively, for the three HC-PBGFs structures.

In summary, for soliton pulse compression, it has been observed that a reduction of the cross-section size of the HC-PBGF results in that the second-order dispersion takes highly-anomalous

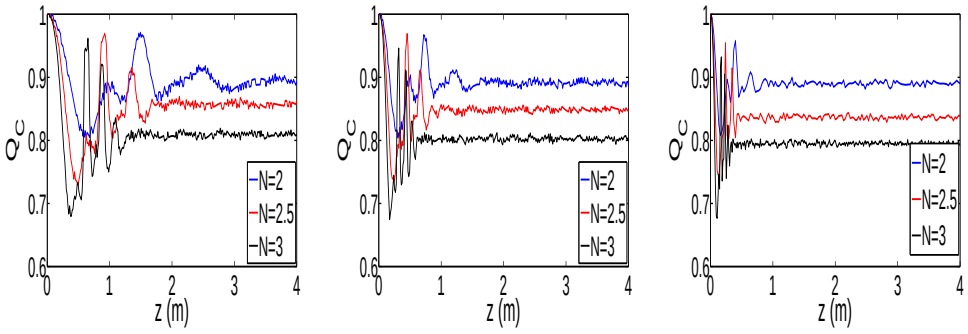

(a) (b) (c)

Fig. 7. Pulse quality factor as a function of propagation length and of soliton number, N, for the studied HC-PBGFs: (a) A, (b) B, and (c) C .

#183383 - $15.00 USD Received 11 Jan 2013; revised 13 Mar 2013; accepted 14 Mar 2013; published 5 Apr 2013

Table 1. Output parameters of the optimum compressed pulse for the studied HC-PBGFs structures.

Structure	N	F_C	Q_C	z_{opt} (cm)
A	2	3.2	0.88	88
	2.5	4.4	0.79	61
	3	5.5	0.72	46
B	2	3.3	0.86	43
	2.5	4.5	0.78	30
	3	5.6	0.71	23
C	2	3.3	0.88	23
	2.5	4.5	0.79	16
	3	5.6	0.73	12

values and, as a consequence, the optimum length for compression is reduced. Our results also show a well known behavior: the greater soliton order (higher power), the higher compression factor that is obtained. This has a cost in the compressed-pulse quality: high values of N results in a reduction in its quality. The impact of the nonlinear parameter on SSFS is clearly visible, since for the same order of soliton, the fiber structure wherein the SSFS is greater is that with the largest nonlinear parameter. On the other hand, it also seen that a larger SSFS is reached, at shorter propagation distance, when the order of the soliton takes greater values and the second-order dispersion is more highly anomalous. The input soliton order, influences on both the SSFS and the amount of energy that will be present in the output pulse, or energy conversion from the input to the output soliton pulse. It is important to note, a high value of the soliton order produces a reduction in the amount of energy contained in shifted soliton pulse. However, the results show that for a value of $N = 3$, the output pulse will contain approximately 80% of the energy of the higher-order input soliton.

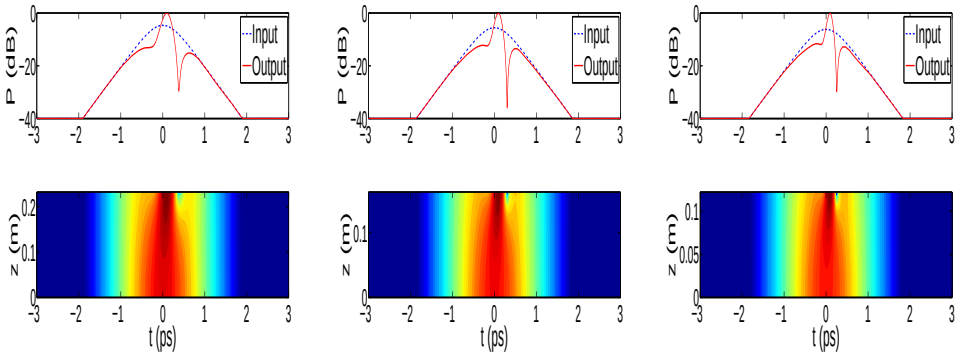

Fig. 8. Upper panels: output compressed pulses as a function of soliton order: (a) $N = 2$, (b) $N = 2.5$ and (c) $N = 3$, for the C fiber structure. Lower panels: corresponding density plots of the temporal evolution of the soliton pulse.

#183383 - $15.00 USD Received 11 Jan 2013; revised 13 Mar 2013; accepted 14 Mar 2013; published 5 Apr 2013

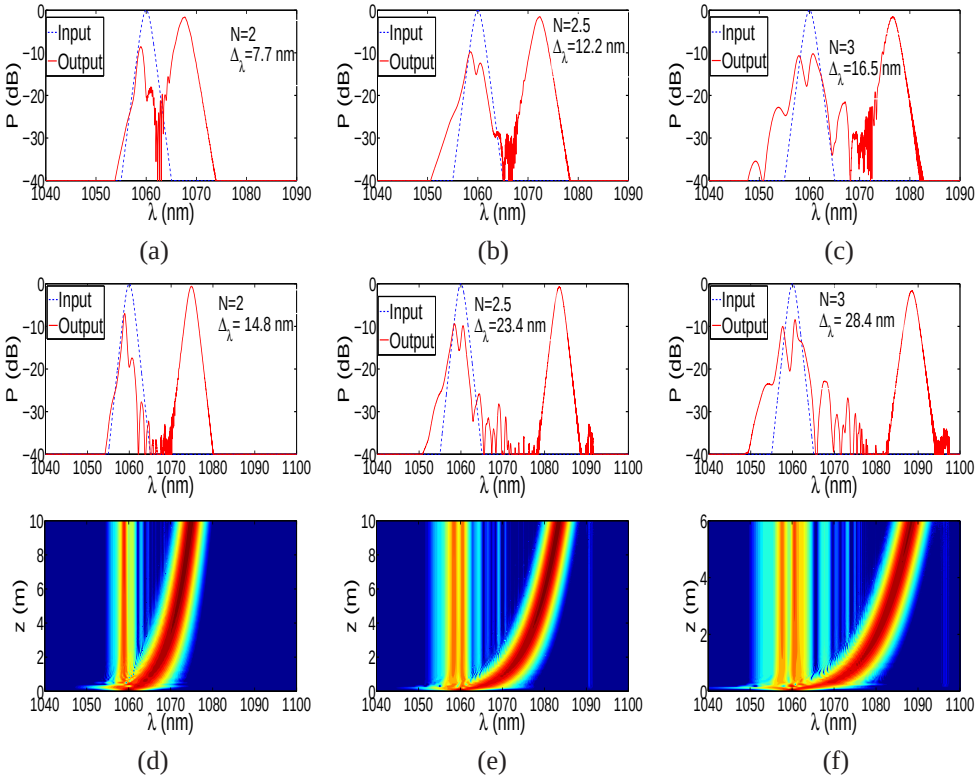

Fig. 9. Spectra of the output-pulse power in the A (a)-(c) and C fiber structures (d)-(f), upper panels. The corresponding density plots (lower panels) for the C fiber structure are also shown. N is the soliton order and Δ_λ is the SSFS. The propagation length is $z = 10$ m except for the case wherein $N = 3$ for the C structure, which $z = 6$ m.

4. Conclusions

We have performed a numerical study of the low-order soliton evolution in three hollow-core photonic bandgap fibers which differ from each other in their cross-section size. We consider unchirped pulses of 400 fs of width and with central wavelength of $\lambda_0 = 1060$ nm. We have focused on the analysis of the pulse quality evolution in soliton pulse compression and soliton self-frequency shift. Our results show that the seven-cell HC-PBGFs, with a cross-section size reduction of 2%, presents larger anomalous values of the second-order dispersion and greater values of the non-linear parameter. If an input soliton pulse with order of $N = 3$ (which corresponds to an energy of 1.69 μJ) propagates a distance of 12 cm, it gets compressed with a compression factor of 5.5 and quality factor of 0.73. Meanwhile, after the input soliton pulse propagates 6 m, its central wavelength redshifts to a shift value of $\Delta_\lambda = 28$ nm and presents a quality factor of ≈ 0.8. This work shows that in both phenomena SPC and SSFS is not only important to have either a high compression factor or a large displacement of the output soliton pulse, respectively, but also a high quality of the output pulse. For the SPC it is desirable that the compressed pulse has the minimum pedestal energy, which implies a high quality factor. On the other hand, in the case of SSFS phenomenon, a high pulse quality results in that most of the energy of the input soliton pulse is transferred to the shifted output soliton pulse. Therefore, an analysis of the pulse quality during the propagation of soliton pulses along HC-PBGFs is

#183383 - $15.00 USD Received 11 Jan 2013; revised 13 Mar 2013; accepted 14 Mar 2013; published 5 Apr 2013

Table 2. Output parameters of the soliton self-frequency shift for the studied HC-PBGFs structures. The propagation length is $z = 10$ m except for the case wherein $N = 3$ for the C structure, which $z = 6$ m.

Structure	N	Δ_λ (nm)	Q_C
A	2	7.7	0.89
	2.5	12.2	0.86
	3	16.5	0.80
B	2	10.6	0.89
	2.5	16.6	0.85
	3	22.4	0.80
C	2	14.8	0.89
	2.5	23.4	0.85
	3	28.4	0.80

necessary in order to find an appropriate fiber structure as well as the input soliton pulse that promotes both SPC and SSFS.

Acknowledgments

NGB acknowledges CONACyT for the scholarship that makes his PhD studies possible. He also acknowledges the InterTech Group from the UV and UPV for allowing him to work with them. We acknowledge CONACyT for partial support, grant 106764 (CB-2008-1). The work of AF was supported by the MINECO TEC2010-15327 grant. The authors would like to thank Carles Milián for useful comments.

#183383 - $15.00 USD Received 11 Jan 2013; revised 13 Mar 2013; accepted 14 Mar 2013; published 5 Apr 2013